JACS
JOURNAL OF THE AMERICAN CHEMICAL SOCIETY

ARTICLE

pubs.acs.org/JACS

Intermolecular Coulombic Decay in Small Biochemically Relevant Hydrogen-Bonded Systems

Spas D. Stoychev,* Alexander I. Kuleff, and Lorenz S. Cederbaum

Theoretische Chemie, PCI, Universität Heidelberg, Im Neuenheimer Feld 229, 69120 Heidelberg, Germany

Supporting Information

ABSTRACT: Intermolecular Coulombic decay (ICD) is a very fast and efficient relaxation pathway of ionized and excited molecules in environment. The ICD and related phenomena initiated by inner-valence ionization are explored for $H_2O\cdots HCHO$, $H_2O\cdots H_2CNH$, $H_2O\cdots NH_3$, $NH_3\cdots H_2O$, $H_2O\cdots H_2S$, $H_2S\cdots H_2O$, and $H_2O\cdots H_2O$ (p-donor$\cdots$p-acceptor). This set of small hydrogen-bonded systems contains seven types of hydrogen bonding, which are typical for biochemistry, and thus its investigation provides insight into the processes that can take place in living tissues. In particular, an estimate of the ICD in biosystems interacting with water (their usual medium) is made. This decay mode is expected to be a source of low-energy electrons proven to be of extreme genotoxic nature. For the purpose of our study, we have used high-precision ab initio methods in optimizing the geometries and computing the single- and double-ionization spectra of formaldehyde−, formaldimine−, ammonia−, hydrogen sulfide−, and water−water complexes. The energy range of the emitted ICD electrons, as well as the kinetic energy of the dissociating ions produced by ICD, is also reported.

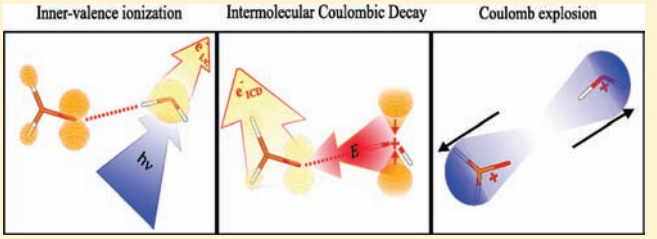

INTRODUCTION

The intermolecular (interatomic) Coulombic decay (ICD)[1] is an extremely efficient electronic decay mode that can be initiated by removal of an electron from the inner-valence shell of an atom or molecule. The thus created ionized and excited system relaxes as an electron from a higher level fills the vacancy and the released energy is transferred to a neighbor from which an electron is ejected. This secondary (ICD) electron usually possesses low energy, of the order of few electron volts. The two positive ions that are formed in the process repel each other, leading typically to a Coulomb explosion of the system. As the charged species fly apart, they do not only break the bond between them. Being highly reactive, these free radicals,[2,3] as well as the low energy electrons (LEE)[4,5] accompanying the decay, can cause a severe damage to any biological system that interacts with them. The ICD process was first theoretically predicted[1] and then confirmed experimentally.[6−8]

An important aspect of the ICD is that it transpires typically on a femtosecond time scale,[9] thus being orders of magnitude faster than the other possible relaxation modes of the system. Excited atoms or molecules can relax via photon emission or, in the case of molecules, also by processes involving nuclear dynamics. However, these processes are usually much slower than ICD and cannot compete with it. In principle, the ICD can be outperformed by the intraatomic or intramolecular autoionization of the initially created electronic state when the latter is energetically allowed. Therefore, if an inner-valence ionized atom or molecule cannot autoionize, but has neighbors, like in a van der Waals[9−11] or in a hydrogen-bonded[12−16] cluster, the system is a prime candidate for ICD. Weak interactions of these kinds are typical in biochemistry, and the ICD is likely to happen in living tissues containing hydrogen-bonded macromolecules.

Our present work is devoted to the study of ICD in small bimolecular systems that contain an oxygen atom as a proton donor or as a proton acceptor. These systems represent the most common types of hydrogen bonding between water and biochemically relevant molecules. We shall later see that the ionization of the inner-valence shell of H_2O triggers ICD in all of the studied species. This result is of great importance, as H_2O makes up more than 70% of the weight of most living organisms. Thus, if a biological object is exposed to an ionizing radiation, the water that it contains will absorb most of it.

As this is the first study of ICD in such systems, we shall not investigate hydrogen-bonded macromolecules, but rather use a set of simple compounds. Because four chemical elements (hydrogen, carbon, nitrogen, and oxygen) make up more than 99% of the mass of most cells, the majority of hydrogen bonds of even the most sophisticated biological system will contain them.[17] By adding sulfur to compare to its weaker bonding and easier ionization, we arrive at a small set of molecular fragments, where the C, N, O, and S atoms are in single and double covalent bonds typical for them (Figure 1a and b). These fragments constitute building blocks common in larger structures like the enzyme lysozyme depicted in Figure 1c.

The simplest systems that incorporate the fragments from Figure 1a are those in which the spare bonds are saturated with hydrogens; see Figure 2. They contain oxygen and can be used to

Received: January 31, 2011
Published: April 12, 2011

   dx.doi.org/10.1021/ja200963y | J. Am. Chem. Soc. 2011, 133, 6817–6824

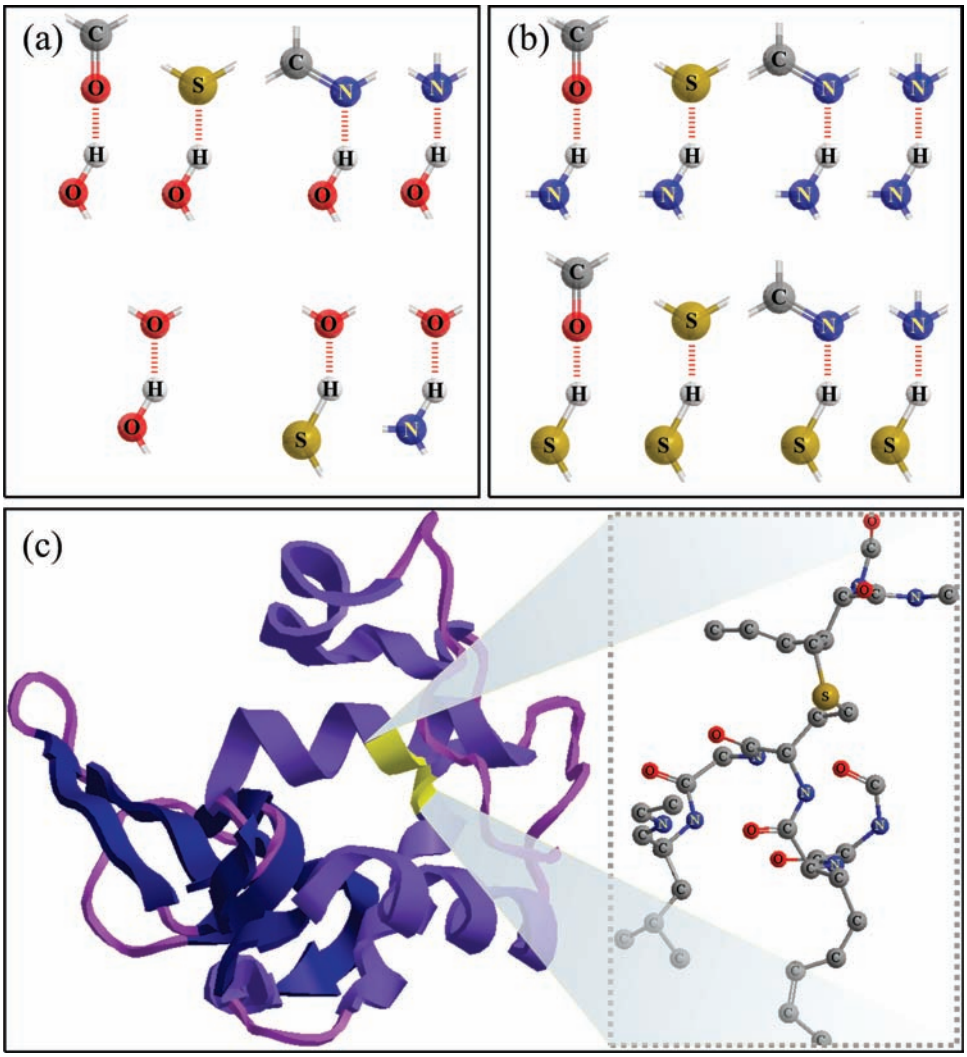

Figure 1. The H-, C-, N-, O-, and S-containing molecular fragments and types of hydrogen bonding (a and b) that are common for the studied $H_2O\cdots HCHO$, $H_2O\cdots H_2CNH$, $H_2O\cdots NH_3$, $NH_3\cdots H_2O$, $H_2O\cdots H_2S$, $H_2S\cdots H_2O$, and $H_2O\cdots H_2O$ (p-donor$\cdots$p-acceptor), as well as for biochemical systems like the enzyme lysozyme (c). For further details, see the text.

investigate the processes characteristic for a macromolecule embedded in water. Working with $H_2O\cdots HCHO$, $H_2O\cdots H_2CNH$, $H_2O\cdots NH_3$, $NH_3\cdots H_2O$, $H_2O\cdots H_2S$, $H_2S\cdots H_2O$, and $H_2O\cdots H_2O$ (p-donor$\cdots$p-acceptor), we can easily analyze the results of our computations and identify the rudimentary effects that govern their interactions. Moreover, if the investigated phenomena are of fundamental nature, they are likely to exist in larger systems, as well. The selected species contain well-known compounds like water, ammonia, formaldehyde, hydrogen sulfide, and formaldimine that should be ideal also for performing experimental studies of the discussed phenomena.

The water dimer is the only system from the chosen set for which the ICD phenomenon has been studied before, both theoretically[12,18,19] and experimentally.[15] It was shown that the ICD is extremely efficient de-excitation mode leading to emission of LEEs. Note that in the experiments carried on water dimer[15] only two intact water ions were observed in the Coulomb explosion following the ICD. This finding indicates that the ICD process is faster than the proton transfer, known itself to be highly efficient with an estimated time scale of less than 50 fs.[20] Moreover, it was confirmed experimentally that the ICD is operative also in big water clusters[16] and is a primary source of genotoxic LEEs produced locally at the vicinity of the radiation absorbing site in the natural environment of the biological macromolecules. Here, analogously, by studying "building blocks" of biomolecules, we provide arguments that the biomolecules themselves can take part in an ICD process, producing LEEs and highly reactive free radicals locally, increasing in this way the probability for inducing further damages of the biosystem.

■ ICD AND OTHER ELECTRONIC DECAY PROCESSES INITIATED BY INNER-VALENCE IONIZATION

The decay phenomena that take place merely due to the presence of neighbors can be successfully investigated by analyzing the character of the initial and the final states of the decay, as shown in refs 1,9−14,21. This amounts to the computation of the electronic spectra of the studied systems and their interpretation. To make this Article comfortable to read, we have put much of the technical details into the Supporting Information. There, the interested reader can find a brief description of the high level ab initio methods used to optimize the geometries and to

dx.doi.org/10.1021/ja200963y |J. Am. Chem. Soc. 2011, 133, 6817–6824

calculate the single- and double-ionization potentials of the studied set of systems.

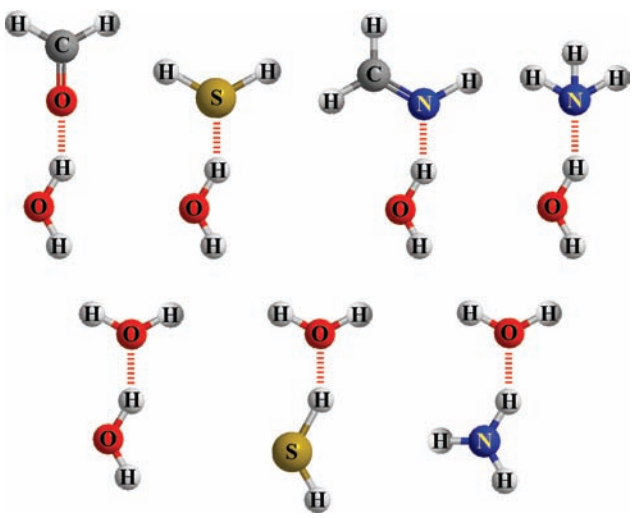

Figure 2. The simplest bimolecular species ($H_2O\cdots HCHO$, $H_2O\cdots H_2CNH$, $H_2O\cdots NH_3$, $NH_3\cdots H_2O$, $H_2O\cdots H_2S$, $H_2S\cdots H_2O$, and $H_2O\cdots H_2O$) that contain the most common types of hydrogen bonding between water and biochemically relevant species. The depicted set incorporates the fragments from Figure 1a with their spare bonds saturated with hydrogen atoms. For further details, see the text.

We shall closely examine one of the selected systems, the water−formaldehyde cluster ($H_2O\cdots HCHO$), as it exhibits all decay modes that are characteristic for the other six species. The systems $H_2O\cdots H_2CNH$, $H_2O\cdots NH_3$, $NH_3\cdots H_2O$, $H_2O\cdots H_2S$, and $H_2S\cdots H_2O$ will be discussed only briefly. More details, like optimized geometries, single- and double-ionization spectra, as well as the spectra of the secondary emitted electrons, can be found in the Supporting Information. The most important features of all of the investigated species, the possible electronic decay channels and the energies of the secondary emitted electrons, are summarized in Table 1. There, an estimate of the kinetic energy release (KER), that is, the sum of the kinetic energy of the two dissociating ions produced by ICD, can also be found. Note that the KER value given is calculated as the Coulomb repulsion of two elementary charges at a distance equal to that between the centers of mass of the hydrogen-bonded subunits at the equilibrium geometry of the cluster. Thus, the possible energy transferred into the internal (vibrational and rotational) degrees of freedom of the ions is not accounted for. One should expect that the KER to be observed in an experiment will have slightly lower values, as shown recently in refs 15 and 18, where the back-to-back flight of the two ions in the Coulomb explosion of $H_2O^+\cdots H_2O^+$ is studied.

$H_2O\cdots HCHO$. The single- and double-ionization spectra of $H_2O\cdots HCHO$ are depicted in panels a and b of Figure 3, respectively. Each vertical line in the spectra corresponds to a cationic state of the system. The position of the line is given by the corresponding ionization energy (or ionization potential),

Table 1. Possible Inter- and Intramolecular Decay Modes of the Inner-Valence (iv) Ionized States of the Studied Species[a]

	processes and energies				
	open channels after the iv ionization of the				
H-bonded system (p-donor···p-acceptor)	p-donor	p-acceptor	products of decay	energy range of the emitted e^- [eV]	maximum in the KER spectrum [eV]
$H_2O\cdots HCHO$	ICD		$H_2O^+/HCHO^+$	0−8	∝4.4
	ETMD[b]		$H_2O\cdots HCHO^{++}$	∝0.0[c]	
		IA	$H_2O\cdots HCHO^{++}$	0−4	
		ICD	$H_2O^+/HCHO^+$	0−10	∝4.4
$H_2O\cdots H_2CNH$	ICD		H_2O^+/H_2CNH^+	0−6	∝4.9
	ETMD[b]		$H_2O\cdots H_2CNH^{++}$	0−2[c]	
		IA	$H_2O\cdots H_2CNH^{++}$	∝0.0[c]	
		ICD	H_2O^+/H_2CNH^+	0−4	∝4.9
$H_2O\cdots NH_3$	ICD		H_2O^+/NH_3^+	0−7	∝4.9
		ICD	H_2O^+/NH_3^+	0−4	∝4.9
$NH_3\cdots H_2O$	ICD		NH_3^+/H_2O^+	0−4	∝4.4
		ICD	NH_3^+/H_2O^+	0−10	∝4.4
		ETMD[b]	$NH_3^{++}\cdots H_2O$	0−2	
$H_2O\cdots H_2S$	ICD		H_2O^+/H_2S^+	0−9	∝4.1
	ETMD[b]		$H_2O\cdots H_2S^{++}$	0−3	
$H_2S\cdots H_2O$		ICD	H_2S^+/H_2O^+	0−11	∝4.2
		ETMD[b]	$H_2S^{++}\cdots H_2O$	0−5	
$H_2O\cdots H_2O$[d]	ICD		H_2O^+/H_2O^+	0−10	4.0[e]
		ICD	H_2O^+/H_2O^+	0−11	4.0[e]

[a] Given are the products of decay, the energies of the emitted secondary electrons, and the positions of the maxima in the kinetic energy release (KER) spectra of the dissociating systems. The abbreviations used are as follows: intermolecular Coulombic decay (ICD), electron-transfer mediated decay (ETMD), and intramolecular autoionization (IA). For further details, see the text and the Supporting Information. [b] Process with low probability. [c] The energy difference is small and could be within or close to the computational error; that is, the channel might be closed. Note that the process might be accomplished through one of the lower in intensity, but higher in energy satellites of the decaying state. [d] See ref 19 where ICD and related processes following inner-valence and core ionization of $H_2O\cdots H_2O$ are studied. [e] The experimental and the computed values are taken from refs 15 and 18, respectively.

dx.doi.org/10.1021/ja200963y |J. Am. Chem. Soc. 2011, 133, 6817–6824

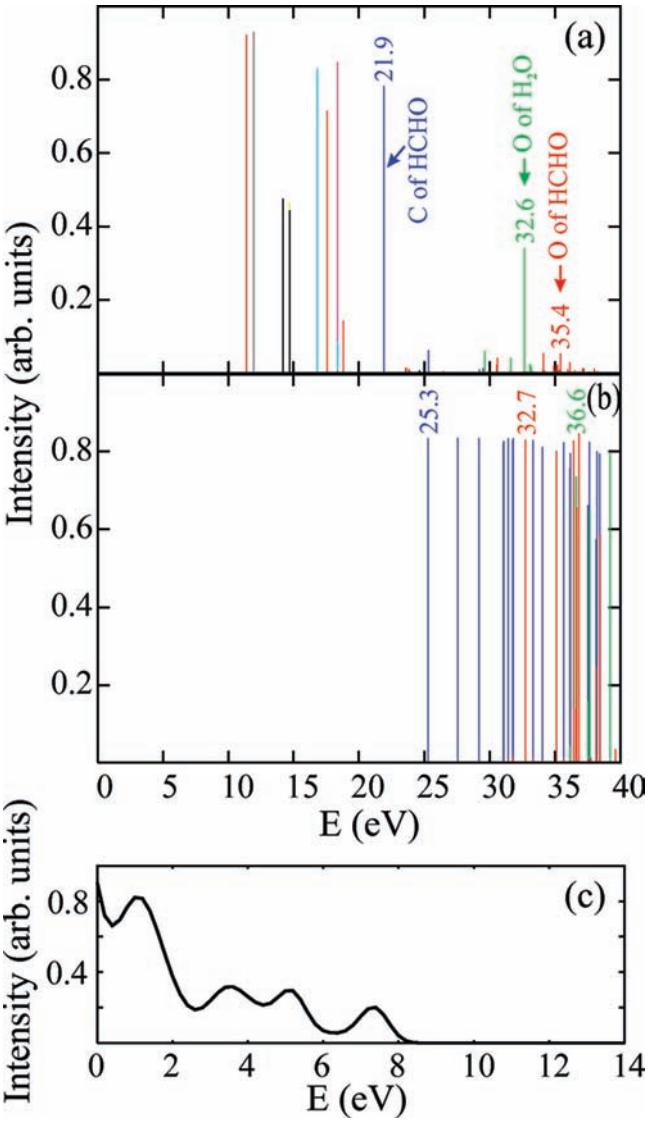

Figure 3. (a and b) Computed single- and double-ionization spectra of $H_2O\cdots HCHO$ in its ground-state equilibrium geometry, respectively. (c) The spectrum of the ICD electron. The colors in (a) indicate the different atoms on which the inner-valence hole is mainly localized, while the colors in (b) indicate the different types of the dicationic states: the two-site states, $H_2O^+\cdots HCHO^+$, are depicted in blue, the one-site states of the type $H_2O^{++}\cdots HCHO$ are depicted in green, and the one-site states of the type $H_2O\cdots HCHO^{++}$ are depicted in red. For further details, see the text and the Supporting Information.

while the hight represents the spectral intensity (related to the ionization cross section[22]). The spectra shown are computed for fixed nuclear geometry (that of the equilibrium state) and thus reflect only the electronic degrees of freedom. That is why the spectra consist of discrete lines. The nuclear degrees of freedom do, of course, influence the ionization spectra introducing a vibrational broadening of the spectral lines reflecting the bonding character of each particular electron with respect to the various normal coordinates of the system. Computing ionization spectra taking into account the vibrational structure is not an easy task, especially for polyatomic systems. However, a fairly good approximation can be obtained by convoluting each line of the spectrum with a Gaussian function with appropriate width to account for the vibrational broadening (see, e.g., ref 23). Here, we will refrain from doing this to make the spectra easier for interpretation, but we will address the issue when it is of relevance.

The ionization potentials (IPs) in Figure 3a can be divided into two groups. Those with energies below 20 eV are states corresponding to ionization out of the outer-valence shell. They lie below the double-ionization threshold of the system of 25.3 eV, which is defined by the lowest in energy line in panel b, and thus cannot decay by electron emission. Their energies and spectral intensities are given in the Supporting Information. The spectral lines above 20 eV are the states stemming from the inner-valence ionization of the system. Most of these states are above the double-ionization threshold and thus can participate in an electronic decay. These are the states that we will concentrate on in the present study. In Figure 3a, these states are depicted with different colors, indicating the different atoms on which the inner-valence vacancy is mainly localized. These are termed as: 2s-type lines of carbon plotted in blue, 2s-type lines of oxygen in water shown in green, and 2s-type lines of oxygen in formaldehyde depicted in red. The two sets of $O2s^{-1}$ states are typical examples of the so-called "breakdown of the molecular orbital picture of ionization"[24] resulting from the strong correlation between the electrons. There, a removal of an electron from a particular molecular orbital (MO) gives rise to a multitude of ionic states forming a quasi-continuum of lines in the spectrum. This behavior is typical for electronically decaying states. The quasi-continuum is actually a discrete representation of the true continuum. In case we were able to use an infinite basis set, each group of states would have formed a single broad spectral line with a Lorentzian shape whose width will correspond to the decay lifetime. The maxima of these broad lines will be centered around the discrete computed states bearing the highest spectral intensities of the corresponding groups. Those states are marked with arrows in Figure 3a.

The lowest in energy dicationic state is at 25.3 eV and relates to the $H_2O^+\cdots HCHO^+$. The IP corresponding to the state stemming from the carbon 2s ionization has energy of 21.9 eV, and hence it cannot take part in an electronic decay process. In contrast, the states corresponding to ionization out of the O2s-type orbitals of both the water and the formaldehyde subunits are above the double-ionization threshold and thus can further decay by electron emission. The lowest in energy dicationic state is of a two-site character ($H_2O^+\cdots HCHO^+$), and, therefore, the decay channels are of intermolecular nature; that is, the respective decay process is ICD.

Let us discuss first the decay process initiated by inner-valence ionization of the water molecule. The lowest in energy one-site dicationic state having two holes on the water molecule is at 36.6 eV (see the lowest in energy green line in Figure 3b); that is, the inner-valence ionized water cannot autoionize. All open decay channels are to two-site dicationic states (blue lines in Figure 3b). Thus, if an electron is removed from the O2s-type orbital of water, an electron from a higher lying orbital of H_2O^+ will fill the O2s vacancy, and an electron from the neighboring HCHO will be ejected. The process can be written in short as:

Step 1 (inner-valence ionization)

$$H_2O\cdots HCHO \xrightarrow{h\nu} H_2O^+(2s^{-1})\cdots HCHO + e^-_{photo}$$

Step 2 (ICD)

$$H_2O^+(2s^{-1})\cdots HCHO \rightarrow H_2O^+(2p^{-1})\cdots HCHO^+(2p^{-1}) + e^-_{ICD}$$

dx.doi.org/10.1021/ja200963y | J. Am. Chem. Soc. 2011, 133, 6817–6824

where the final hole on the water molecule will be in an orbital consisting mainly of the 2p MO of the oxygen, while the hole on formaldehyde will be in an orbital constructed from the 2p MOs of the carbon and oxygen.

Because the hydrogen bond is very weak, the repulsion between the two positive charges produced by the ICD process on the two hydrogen-bonded species will lead to a Coulomb explosion of the system. The kinetic energy release of the exploding H_2O^+ and $HCHO^+$ can be estimated assuming that ICD is much faster than the nuclear motion of the heavier atoms in the cluster. Considering the 3.3 Å distance between the centers of mass of the hydrogen-bonded H_2O and HCHO, a value of 4.4 eV for the KER is expected. However, as mentioned above, the Coulomb repulsion energy can also be partly distributed among the rotational and vibrational degrees of freedom of the ions produced, and thus in reality the maximum in the KER spectrum would appear at lower energies. In the case of the Coulomb explosion following the ICD in $H_2O\cdots H_2O$, this effect yields a decrease of the KER as compared to the rigid species approximation by about 0.6 eV.[15,18]

The ICD in $H_2O\cdots$HCHO initiated by inner-valence ionization of the water molecule is schematically represented in the left-hand-side panels of Figure 4. The right-hand-side panels of the same figure show the ICD process that might take place in a carbonyl-containing fragment of the enzyme lysozyme hydrogen bonded with H_2O. The ultrafast decay by ICD should be observed in both the water−formaldehyde cluster and the surrounded by water biochemical macromolecule. The mechanism of the decay will be the same in both cases, as was also found to be in water dimer and large water clusters.[15,16] However, due to the much larger number of vibrational and rotational modes in which the excess energy of the final states can be distributed, the production of the two positively charged species will not necessarily lead to a Coulomb explosion and disintegration of the macromolecule but probably rather to a local bond breaking and to a "heating up" of the system. The low-energy electrons and the radicals produced are expected to further induce damages in the biosystem.

Let us now turn to the question of the energy distribution of the emitted ICD electrons. To compute a decay-electron spectrum, one needs first to construct the full potential energy hypersurfaces of the initial state, the intermediate decaying states, and the final states. In the case of the discussed ICD, these are the neutral ground state, the singly ionized states, and the doubly ionized states of the system. In addition, one needs to compute the partial decay widths of each decaying state as a function of the nuclear degrees of freedom and perform nuclear wavepacket dynamics calculations to describe the decay process. Even for diatomics such calculations are notoriously difficult.[25] For polyatomics, they are far beyond reach of any current theoretical method. However, our experience with the ICD-electron spectrum of water dimer[12,19] shows that only the data from the single- and double-ionization spectra of the system in its equilibrium geometry suffice to obtain ICD-electron spectra in a fairly good agreement with the experimental results.[15] This can be done by using spectral envelopes to account for the vibrational structure of the initial and final for the decay states. The spectral envelopes can be calculated by convoluting each individual line by a Gaussian with an appropriate full width at half-maximum (fwhm). Assuming that the probability of the transitions is independent of the energy differences between the initial and the final state, the kinetic energy distribution of the emitted electrons can then be derived by convoluting the single- and

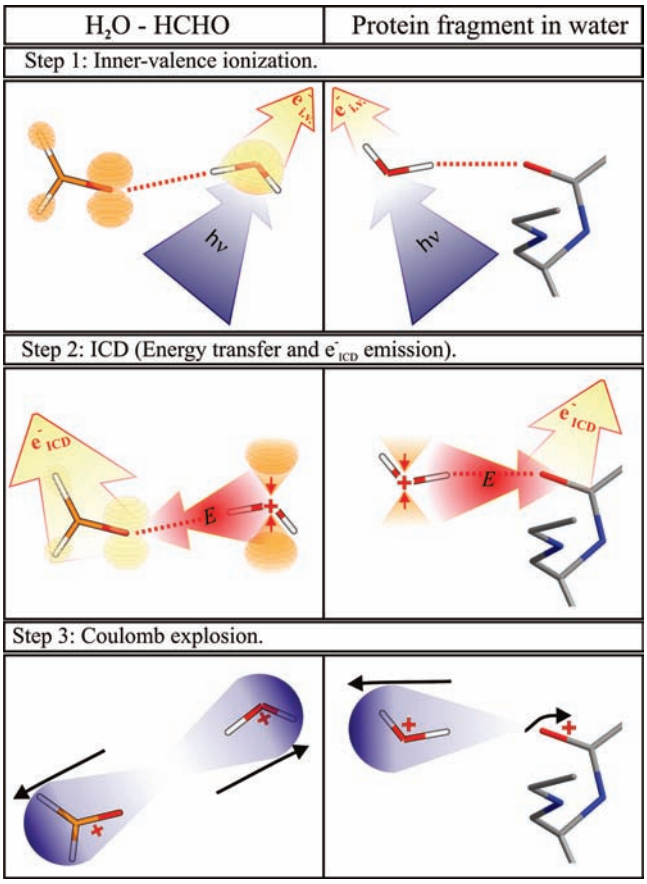

Figure 4. Schematic representation of the intermolecular Coulombic decay in $H_2O\cdots$HCHO (left) and in a H_2O interacting with a fragment from the enzyme lysozyme (right). The ICD process is initiated by an inner-valence ionization of the water molecule (upper panels). The created vacancy is filled by an electron from a higher lying electronic shell of the same unit, and a secondary electron is emitted from the neighboring unit (middle panels). In the case of $H_2O\cdots$HCHO, a Coulomb explosion follows, as the two positively charged species fly apart, and a bond breaking and a restructuring of the macromolecule follows in the case of the lysozyme−water complex (lower panels). The produced low-energy ICD electrons and radicals may induce further damages of the biosystem. For more details, see the text.

double-ionization spectral envelopes and accounting for the proper weighting of the open decay channels:

$$S(E) = \frac{\int_0^\infty S_{in}(E-E')S_{fin}(E')\,dE'}{\int_0^E S_{fin}(E')\,dE'} \quad (1)$$

In eq 1, $S_{in}(E)$ is the spectral envelope of the singly ionized system, and $S_{fin}(E)$ is the spectral envelope of the two-site doubly ionized system. To obtain correctly the weights of the different channels, one has to normalize to the initial population, because, otherwise, decay channels from higher in energy states that are always open will artificially get more weight than channels that are closed from some energy on. In the above expression, this is accounted for by dividing the spectral convolution by the appropriate energy-dependent wight.

The kinetic-energy distribution of the electrons ejected in the ICD of $H_2O\cdots$HCHO obtained via the above procedure using

dx.doi.org/10.1021/ja200963y |J. Am. Chem. Soc. 2011, 133, 6817–6824

a fwhm of 0.7 eV is shown in Figure 3c. The spectrum has a maximum at 0 eV followed by a drop in the intensity, suggesting that the emitted e^-_{ICD} will have energies between 0 and 8 eV with more than one-half of them with energy below 3 eV. We would like to note that the spectrum is not very sensitive to the particular choice of the width of the Gaussian envelopes. Choosing smaller fwhm values will lead to a more structured spectrum, while larger ones will lead to a smoother drop off of the electron-energy distribution. Most likely, a measured ICD spectrum will be less structured than the one depicted in Figure 3c as the comparison between the ICD-electron spectrum of the water dimer computed via the above procedure[12,19] and the one obtained experimentally[15] shows.

The process described above is characterized by a transfer of energy from the initially ionized unit to its neighbor. This is the dominant relaxation mode of $H_2O^+(2s^{-1})\cdots HCHO$ due to its very high efficiency. However, the discovery of ICD revealed a whole plethora of related phenomena (see, e.g., refs 11,26−29). Important for the present study is also the interatomic decay process in which an electron transfer mediates the decay, the so-called electron-transfer-mediated decay (ETMD).[11,21,30,31] There, the inner-valence vacancy is refilled by an outer-valence electron of the neighbor, from which a secondary electron is emitted. Thus, in contrast to ICD, the system ends up with two vacancies on a site different from the initially ionized one. Involving an electron transfer, the ETMD is naturally much slower than the ICD and has a real impact on the decay of the system only if no ICD channel is open, as shown for NeAr in ref 11. Nevertheless, we shall discuss the possibility of electron-transfer mediated decay in the water−formaldehyde cluster for completeness.

According to our calculations, the position of the main line of $H_2O^+(2s^{-1})\cdots HCHO$ is just one tenth of eV below that of the lowest in energy $H_2O\cdots HCHO^{++}$ state. This doubly ionized one-site state of $H_2O\cdots HCHO$ in which two electrons are removed from the formaldehyde molecule is at 32.7 eV; see Figure 3b. One has to bear in mind that this small energy difference is within the error of the computational methods used, and even if we take into account that the lines shown in Figure 3b will acquire widths due to the nuclear degrees of freedom, as discussed above, we cannot definitely say whether ETMD takes place here. For that, even more accurate calculations would be necessary. Nevertheless, we would like to briefly discuss our results on ETMD noting that it is beyond doubt possible for other members of our set of molecules (see Table 1 and text below). After the creation of a vacancy in an O2s-type MO of H_2O, an electron from the neighboring subunit can fill it, and another (ETMD) electron can be ejected from the initially neutral HCHO. In short:

$$H_2O^+(2s^{-1})\cdots HCHO \rightarrow H_2O\cdots HCHO^{++}(2p^{-2}) + e^-_{ETMD}$$

Here, the energy of the emitted electron is expected to be close to 0 eV, and the created $H_2O\cdots HCHO^{++}$ will, of course, not undergo a Coulomb explosion. The ETMD process will compete with the much more probable ICD, and thus only a minor fraction of the initially populated $H_2O^+(2s^{-1})\cdots HCHO$ will undergo an electron-transfer -mediated decay.

Let us now turn to the processes that can be initiated by inner-valence ionization of the formaldehyde, the $H_2O\cdots HCHO^+$-$(2s^{-1}$ of O) states. As seen in Figure 3a, the most intense respective line in the ionization spectrum is at 35.4 eV and is higher in energy than both the $H_2O^+\cdots HCHO^+$ and the $H_2O\cdots HCHO^{++}$ thresholds shown in Figure 3b. This means that the inner-valence ionized HCHO can undergo intermolecular decay, that is, ICD, as well as an intramolecular autoionization. Starting from the inner-valence (O2s-type) ionization of formaldehyde:

Step 1 (inner-valence ionization)

$$H_2O\cdots HCHO \xrightarrow{h\nu} H_2O\cdots HCHO^+(2s^{-1}\text{of O}) + e^-_{photo}$$

the system can undergo the following decay processes.

Step 2 (intramolecular autoionization (IA) and ICD):

$$H_2O\cdots HCHO^+(2s^{-1}\text{of O}) \begin{cases} \nearrow & H_2O\cdots HCHO^{++}(2p^{-2}) + e^-_{IA}. \\ \searrow & H_2O^+(2p^{-1}) + HCHO^+(2p^{-1}) + e^-_{ICD}. \end{cases}$$

The formation of $H_2O\cdots HCHO^{++}$ by intramolecular autoionization will be accompanied by the emission of a secondary electron with energies between 0 and 4 eV, while the formation of $H_2O^+\cdots HCHO^+$ by ICD will produce electrons with energies between 0 and 10 eV. To estimate the relative importance of these intra- and intermolecular decays, a detailed computation of the decay rates for these processes is needed, which is currently not possible. In general, intramolecular electronic decay processes are expected to be faster than the intermolecular ones, and, thus, we assume the intramolecular autoionization process to outperform its intermolecular competitor. However, because the produced ionic fragments by intramolecular autoionization and ICD differ, the two electronic decay modes could be, in principle, separated and their weights measured in an experiment.

$H_2O\cdots H_2CNH$, $H_2O\cdots NH_3$, $NH_3\cdots H_2O$, $H_2O\cdots H_2S$, and $H_2S\cdots H_2O$. We will continue our discussion with a short description of the decay processes in the other systems that have been investigated. As already mentioned, the results of our computations are summarized in Table 1, while more details, like ionization and secondary electron spectra, are given in the Supporting Information.

The presence of the π-bond in $H_2O\cdots H_2CNH$ makes its properties similar to those of the water−formaldehyde cluster studied in the previous section. In particular, low single- and double-ionization thresholds are a characteristic feature of the system, and the IPs of the carbon 2s-type states are below the double-ionization threshold of $H_2O\cdots H_2CNH$ (see Table S3 and Figure S3 in the Supporting Information). The spectral lines stemming from the ionization of the O2s-type MO have energies above 29 eV with the most intense line at 32.6 eV. These states are well above the lowest $H_2O^+\cdots H_2CNH^+$ state located at 26.1 eV, and thus an ICD process can be initiated by inner-valence ionization of the water molecule. The $H_2O^+(2s^{-1})\cdots H_2CNH$ could also undergo ETMD, but it will compete with the much more efficient ICD and can be neglected. ICD processes can be initiated also from inner-valence ionization of H_2CNH, from the state $H_2O\cdots H_2CNH^+(2s^{-1}$ of N). The spectral lines related to the ionization of the N2s orbital are above 27 eV with the most intense line at about 30.6 eV. Although our computations show that the channel for intramolecular autoionization is closed for the most intense $H_2O\cdots H_2CNH^+(2s^{-1}$ of N) line, for some higher lying states populated by the ionization of the nitrogen 2s-type MO, the intramolecular autoionization channel is open.

Let us turn now to $H_2O\cdots NH_3$ (see Figure S4 in the Supporting Information). Our computations show that for this

system the ICD process can be initiated by inner-valence ionization of both the H_2O and the NH_3 subunits. The most intense line of $H_2O^+(2s^{-1})\cdots NH_3$ is at 31.7 eV, and that of $H_2O\cdots NH_3^+(2s^{-1})$ at 28.0 eV, while the lowest in energy doubly ionized two-site state is positioned at 26.7 eV. There are no ETMD or intramolecular autoionization channels open; thus ICD appears as the only possible electronic decay mode.

The water and ammonia molecules can also bind such that NH_3 is the proton donor and H_2O the proton acceptor; see Figure 2. In this case, removing an electron form the inner-valence nitrogen 2s-type MO will again lead to ICD. However, the inner-valence ionization of the water subunit gives rise not only to ICD, but also to ETMD. The intramolecular autoionization channels are closed in all cases; that is, inner-valence ionized states of $NH_3\cdots H_2O$ can decay only by intermolecular mechanisms.

The water−hydrogensulfide complex is characterized by a very week hydrogen bond. In the case of H_2O being the proton donor, it is more than 2.5 Å long, while in the case of H_2O being the proton acceptor it is about 2.1 Å. In both cases, the bond is significantly longer than that in the other systems studied (see Figure S1). As a consequence of the large distance between the constituents, the two-site double-ionization threshold is lower due to the reduced Coulomb repulsion energy between the H_2O^+ and H_2S^+ ions. Nevertheless, because the inner-valence shell of H_2S is a 3s-type MO, the resulting respective ionic states lie relatively low in energy, and the ICD from $H_2S^+(3s^{-1})$ is energetically forbidden (see Figures S6 and S7, as well as Tables S6 and S7 in the Supporting Information). The inner-valence ionized water, however, can decay both by ICD and ETMD to $H_2O^+\cdots H_2S^+$ and $H_2O\cdots H_2S^{++}$, respectively.

Finally, we briefly comment on the implications of the studied processes in more complex systems. As mentioned already, the electronic decay processes that take place in the small hydrogen-bonded systems studied will be operative in large biological macromolecules in aqueous environment as well. The inner-valence ionization of a water molecule bonded to a macromolecule will always lead to ICD (see Figure 4) as the most efficient relaxation pathway. In the case of inner-valence ionization of the macromolecule participating in the hydrogen bond, the ICD will also be operative (except if the electronic state is low in energy like in H_2S), but depending on the covalent structure of this subunit, it may have to compete with the possibly more efficient intramolecular autoionization. The π-bonded structures typically possess low first single and double IPs and relatively high single inner-valence IPs. Our results show (see Table 1) that intramolecular autoionization will be most likely energetically open for such systems. For all other types of covalent bonding, the intramolecular autoionization channel will be most likely closed, and thus the ICD will be the only possible mechanism of electronic decay.

■ CONCLUSION

Ultrafast intermolecular decay processes in water containing hydrogen-bonded systems, where the H_2O molecule is a p-donor or a p-acceptor, have been investigated. In particular, the most efficient relaxation modes of the inner-valence ionized $H_2O\cdots HCHO$, $H_2O\cdots H_2CNH$, $H_2O\cdots NH_3$, $NH_3\cdots H_2O$, $H_2O\cdots H_2S$, $H_2S\cdots H_2O$, and $H_2O\cdots H_2O$ (p-donor$\cdots$p-acceptor) have been established. The selected systems represent seven types of hydrogen bonding that are the most commonly formed between water and macromolecules in biochemistry. In addition to the identification of the processes, the energies of the emitted secondary electrons and of the kinetic energy released by the created ions have been estimated.

In the course of our study, the geometries of the examined clusters have been optimized using MP2 method and large basis sets. The resulting structures are characterized by hydrogen bonds in the range from 1.942 to 2.515 Å and are used as input data in Green's function-based computations of their single- and double-ionization spectra. To the best of our knowledge, the ionization spectra of $H_2O\cdots HCHO$, $H_2O\cdots H_2CNH$, $H_2O\cdots NH_3$, $NH_3\cdots H_2O$, $H_2O\cdots H_2S$, and $H_2S\cdots H_2O$ calculated with such a high precision have not been reported in the literature.

Our results demonstrate that ICD will take place in all of the selected species. In particular, the inner-valence ionization of the water molecule in each of the studied systems will be followed by the very fast and efficient ICD. Inner-valence ionization of the H_2O molecule produces decay channels, which are open by several eV; therefore, this relaxation mode will also be operative in larger systems containing hydrogen-bonding types of the investigated set. The electronic and steric effects typical for macromolecules are not expected to modify this qualitative result. Although the presence of other water molecules of the environment and of that part of the biomolecule that does not participate in the hydrogen bond will change the ionization potentials of the species forming the hydrogen bond, we expect that these changes will be insufficient to close the energy gap between the initial and final states of the intermolecular decay. Moreover, theoretical and experimental studies[32−34] show that the ionization potentials of DNA and RNA bases in aueous solution are lower as compared to those in the gas phase, which will actually facilitate the ICD channels identified in the present study. That is, the eminent presence of water surrounding the biological objects and the relatively high energy of its inner-valence ionized states guarantee that ICD will take place. Consequently, LEEs and radical cations will be produced. These products of the ICD process may further create damages of the biomolecule, as shown in refs 2−5; see also refs 10,15,16.

At the end, we would like to comment on the practical importance of the discussed ICD process. Becuse ICD appears as a primary source of genotoxic particles (LEEs and cationic radicals), it is clear that a detailed knowledge of this fundamental process may help in finding mechanisms to control it. For example, the ICD channel in ammonia clusters can be closed by protonation of the ammonia, as was shown very recently.[35] Importantly, the low-energy ICD electrons and the cationic radicals are produced at the site of the biosystem that participates in the ICD process, that is, where the incoming photon was absorbed. Hence, the damages will be most probably induced in a close proximity of this site. This feature may also be probably used in practice. By adding a suitable constituent opening the ICD channel, one may produce LEE locally on the probe that may subsequently damage some undesirable part of the biosystem. In the long run, one may imagine using this feature of the ICD even in medicine.

We hope that our results will stimulate further experimental and theoretical studies on the important and fascinating subject of intermolecular Coulombic decay.

■ ASSOCIATED CONTENT

Supporting Information. Complete ref 15 as well as a brief description of the computational methods used; optimized

geometries; single- and double-ionization spectra; possible electronic decay mechanisms after inner-valence ionization; and ICD-electron spectra of the systems $H_2O\cdots H_2CNH$, $H_2O\cdots NH_3$, $NH_3\cdots H_2O$, $H_2O\cdots H_2S$, and $H_2S\cdots H_2O$. This material is available free of charge via the Internet at http://pubs.acs.org.

AUTHOR INFORMATION

Corresponding Author
spas.stoychev@pci.uni-heidelberg.de

ACKNOWLEDGMENT

The research leading to these results has received funding from the European Research Council under the European Community's Seventh Framework Programme (FP7/2007-2013)/ERC Advanced Investigator Grant no. 227597.

REFERENCES

(1) Cederbaum, L. S.; Zobeley, J.; Tarantelli, F. *Phys. Rev. Lett.* **1997**, *79*, 4778.
(2) O'Neill, P.; Stevens, D. L.; Garman, E. F. *J. Synchrotron Radiat.* **2002**, *9*, 329.
(3) Purkayastha, S.; Milligan, J. R.; Bernhard, W. A. *J. Phys. Chem. B* **2005**, *109*, 16967.
(4) Boudaïffa, B.; Cloutier, P.; Hunting, D.; Huels, M. A.; Sanche, L. *Science* **2000**, *287*, 1658.
(5) Martin, F.; Burrow, P. D.; Cai, Z.; Cloutier, P.; Hunting, D.; Sanche, L. *Phys. Rev. Lett.* **2004**, *93*, 068101.
(6) Marburger, S.; Kugeler, O.; Hergenhahn, U.; Möller, T. *Phys. Rev. Lett.* **2003**, *90*, 203401.
(7) Jahnke, T.; Czasch, A.; Schöffler, M. S.; Schössler, S.; Knapp, A.; Käsz, M.; Titze, J.; Wimmer, C.; Kreidi, K.; Grisenti, R. E.; Staudte, A.; Jagutzki, O.; Hergenhahn, U.; Schmidt-Böcking, H.; Dörner, R. *Phys. Rev. Lett.* **2004**, *93*, 163401.
(8) Öhrwall, G.; Tchaplyguine, M.; Lundwall, M.; Feifel, R.; Bergersen, H.; Rander, T.; Lindblad, A.; Schulz, J.; Peredkov, S.; Barth, S.; Marburger, S.; Hergenhahn, U.; Svensson, S.; Björneholm, O. *Phys. Rev. Lett.* **2004**, *93*, 173401.
(9) Santra, R.; Zobeley, J.; Cederbaum, L. S. *Phys. Rev. B* **2001**, *64*, 245104.
(10) Müller, I. B.; Cederbaum, L. S. *J. Chem. Phys.* **2005**, *122*, 094305.
(11) Zobeley, J.; Santra, R.; Cederbaum, L. S. *J. Chem. Phys.* **2001**, *115*, 5076.
(12) Müller, I. B.; Cederbaum, L. S. *J. Chem. Phys.* **2006**, *125*, 204305.
(13) Santra, R.; Cederbaum, L. S.; Meyer, H.-D. *Chem. Phys. Lett.* **1999**, *303*, 413.
(14) Santra, R.; Zobeley, J.; Cederbaum, L. S.; Tarantelli, F. *J. Electron Spectrosc. Relat. Phenom.* **2001**, *114−116*, 41.
(15) Jahnke, T.; et al. *Nat. Phys.* **2010**, *6*, 139.
(16) Mucke, M.; Braune, M.; Barth, S.; Förstel, M.; Lischke, T.; Ulrich, V.; Arion, T.; Becker, U.; Bradshaw, A.; Hergenhahn, U. *Nat. Phys.* **2010**, *6*, 143.
(17) Nelson, D. L.; Cox, M. M. *Lehninger Principles of Biochemistry*; W.H. Freeman: New York, 2014.
(18) Vendrell, O.; Stoychev, S. D.; Cederbaum, L. S. *ChemPhysChem* **2010**, *11*, 1006.
(19) Stoychev, S. D.; Kuleff, A. I.; Cederbaum, L. S. *J. Chem. Phys.* **2010**, *133*, 154307.
(20) Furuhama, A.; Dupuis, M.; Hirao, K. *J. Chem. Phys.* **2006**, *124*, 164310.
(21) Averbukh, V.; Müller, I. B.; Cederbaum, L. S. *Phys. Rev. Lett.* **2004**, *93*, 263002.
(22) Cederbaum, L. S.; Domcke, W. *Adv. Chem. Phys.* **1977**, *36*, 205.
(23) Lichtenberger, D. L.; Copenhaver, A. S. *J. Electron Spectrosc. Relat. Phenom.* **1990**, *50*, 335.
(24) Cederbaum, L. S.; Domcke, W.; Schirmer, J.; von Niessen, W. *Adv. Chem. Phys.* **1986**, *65*, 115.
(25) Sisourat, N.; Kryzhevoi, N. V.; Kolorenč, P.; Scheit, S.; Jahnke, T.; Cederbaum, L. S. *Nat. Phys.* **2010**, *6*, 508.
(26) Santra, R.; Cederbaum, L. S. *Phys. Rev. Lett.* **2003**, *90*, 153401.
(27) Barth, S.; Joshi, S.; Marburger, S.; Ulrich, V.; Lindblad, A.; Öhrwall, G.; Björneholm, O.; Hergenhahn, U. *J. Chem. Phys.* **2005**, *122*, 241102.
(28) Aoto, T.; Ito, K.; Hikosaka, Y.; Shigemasa, E.; Penent, F.; Lablanquie, P. *Phys. Rev. Lett.* **2006**, *97*, 243401.
(29) Gokhberg, K.; Trofimov, A. B.; Sommerfeld, T.; Cederbaum, L. S. *Europhys. Lett.* **2005**, *72*, 228.
(30) Sakai, K.; Stoychev, S.; Ouchi, T.; Higuchi, I.; Schöffler, M.; Mazza, T.; Fukuzawa, H.; Nagaya, K.; Yao, M.; Tamenori, Y.; Kuleff, A. I.; Saito, N.; Ueda, K. *Phys. Rev. Lett.* **2011**, *106*, 033401.
(31) Forstel, M.; Mucke, M.; Arion, T.; Bradshaw, A. M.; Hergenhahn, U. *Phys. Rev. Lett.* **2011**, *106*, 033402.
(32) Crespo-Hernández, C. E.; Arce, R.; Ishikawa, Y.; Gorb, L.; Leszczynski, J.; Close, D. M. *J. Phys. Chem. A* **2004**, *108*, 6373.
(33) Belau, L.; Wilson, K. R.; Leone, S. R.; Ahmed, M. *J. Phys. Chem. A* **2007**, *111*, 7562.
(34) Slavček, P.; Winter, B.; Faubel, M.; Bradforth, S. E.; Jungwirth, P. *J. Am. Chem. Soc.* **2009**, *131*, 6460.
(35) Kryzhevoi, N. V.; Cederbaum, L. S. *Angew. Chem., Int. Ed.* **2011**, *50*, 1306.